energies

MDPI

Article

Experimental Determination of Parameters of Nonlinear Electrical Load

Aleksandr Skamyin [1,*], Yaroslav Shklyarskiy [2], Vasiliy Dobush [2] and Iuliia Dobush [2]

1 Department of Electric Power and Electromechanics, Saint-Petersburg Mining University, 199106 Saint-Petersburg, Russia
2 Department of General Electrical Engineering, Saint-Petersburg Mining University, 199106 Saint-Petersburg, Russia; Shklyarskiy_YaE@pers.spmi.ru (Y.S.); dobush_vs@pers.spmi.ru (V.D.); Rastvorova_YuV2@pers.spmi.ru (I.D.)
* Correspondence: skamin_AN@pers.spmi.ru

Abstract: The paper deals with issues of modeling nonlinear electrical loads of various types, such an uncontrolled rectifier, thyristor rectifier, thyristor power regulator and mixed equivalent nonlinear load. For these load types, existing analytical expressions were identified to determine the magnitudes of harmonic currents, and waveforms of currents were obtained during measurements in laboratory conditions with variable parameters of the grid impedance and load. The obtained results were compared, and it was found that the error in determining the magnitudes of harmonic currents can reach 60% for an individual load and 54% for an equivalent load. A more accurate method for determining the parameters of nonlinear electrical load is also proposed, which is based on the application of shunt harmonic filters. In laboratory conditions, it was found that when using the developed method, the error did not exceed 10% for an individual load and 14% for an equivalent load.

Keywords: harmonics; total harmonic distortion; power quality; nonlinear electrical load; capacitor banks; passive filters; experimental study; six-pulse rectifier; thyristor regulator; modeling

check for updates

Citation: Skamyin, A.; Shklyarskiy, Y.; Dobush, V.; Dobush, I. Experimental Determination of Parameters of Nonlinear Electrical Load. *Energies* **2021**, *14*, 7762. https://doi.org/10.3390/en14227762

Academic Editor: Tek Tjing Lie

Received: 21 October 2021
Accepted: 15 November 2021
Published: 19 November 2021

1. Introduction

In modern industrial power supply systems, there has been a significant increase in the installed capacity of nonlinear electric loads, for example, a lot of nonlinear load types are used in the mining industry [1] and railway traction power systems [2], and arc furnaces are powered by rectifiers [3]. Renewable energy sources must be provided with semiconductor devices [4,5]. At the same time, measures to minimize the electromagnetic interference that such power supply systems generate are not being widely implemented. The operation of such devices is characterized by nonsinusoidal current consumption, which leads to the appearance of supply voltage harmonics. On the one hand, the implementation of this kind of electrical equipment leads to an increase in energy efficiency [6,7] and the automation of technological processes. On the other hand, in the absence of additional compensation measures, it negatively affects the operation of other electrical receivers, circuit protection devices and communication devices, and can lead to downtime and losses in production, as well as to difficulties in determining power consumption [8]. There are known cases of stoppages in technological lines at food industry enterprises resulting from exceeding the voltage distortion levels due to outside, nonlinear consumers being connected to the point of common coupling [9]. So, it is necessary to provide power quality indices control [10,11] in order to both identify power distortion sources [12] and compensate for the resulting harmonics [13].

To carry out calculations and an analysis of nonsinusoidal modes of consumer operation, it is necessary to use correct equivalent circuits for linear and nonlinear electrical loads, which makes it possible to determine harmonic emissions and distributions in the electrical network with sufficient accuracy. This question is relevant when choosing the parameters

of devices that improve power quality and compensate for harmonic distortions in voltage and current [14,15]. In this case, the validity of nonsinusoidal mode modeling is supported by the adopted model of the nonlinear electrical load.

Representations of nonlinear electrical loads by nonlinear current-voltage characteristics, approximated by various functions, are widespread, for example, switching functions [16] or differential equations [17,18]. However, more sophisticated approaches based on semiconductor converter models have also been extensively used [19]. The complexity of mathematical models leads to the limited use of analytical methods [20,21] and more extended use of simulation modeling, which makes it possible to obtain numerical solutions for the tasks [22,23]. In addition, it is often necessary to carry out rough estimates of network operation modes with nonlinear loads while maintaining sufficient accuracy for engineering practice. In this case, the calculations can be quite approximate, and do not require the application of complex mathematical models. Traditional modelling of nonlinear load seems to be suitable in this case [24,25].

In [24,26,27], diode six-pulse rectifier modelling is considered. Such a model, represented by current sources with magnitude I_h, may be calculated by the Equation:

$$I_h = \frac{I_1}{h} \tag{1}$$

where h is the harmonic order and I_1 is the magnitude of the first harmonic current consumed by the rectifier. The advantage of this model is the simplicity of its application; however, such a model is inaccurate [28], and the legitimacy of its use has, in many cases, been questioned. According to [29,30], it is also common to represent the diode six-pulse rectifier as a source of current harmonics, as determined by the current spectrum.

In addition, the model of diode six-pulse rectifier can be presented by means of a table based harmonic model [24,31]. The table is created based on experimental measurements of the rectifier currents when external conditions are changing (e.g., line impedance, additional ac-reactance, dc-link inductance and load parameters). A wide range of reference information increases the accuracy of the calculations, but this approach is very time consuming when measuring large amounts of data.

A number of articles [32,33] have proposed representing nonlinear loads on the basis of time-domain [34,35], harmonic domain [36] or frequency domain models [37]. According to the frequency-domain model approach, a power converter may be analyzed by observing the converter passing through a sequence of states describing its conduction pattern. In each state, the converter can be represented by a passive linear circuit and analyzed with the help of complex harmonic phasors [38,39]. As for the time domain model, the converter is represented by a system of differential equations or operating state equations [40–42]. After solving these equations, the spectrum of the converter harmonic currents from the AC side is determined using the fast Fourier transform.

One of the most widespread approached in harmonic power flow is the hybrid time-frequency domain method. It tries to exploit the advantages of the time and frequency domain approaches, i.e., linear components are modeled in the frequency-domain, while nonlinear components are represented in the time-domain [17,26,27,43].

According to [25], for thyristor power regulators, the 2nd, 3rd, 4th, 5th, 7th, 11th, 13th harmonic currents are the most typical (more than 0.5%). In the case of an individual consumer, the magnitudes of 5th, 7th, 11th, 13th harmonics are determined by the following equation:

$$I_h = \frac{0.7S_{nom}}{\sqrt{3}U_{nom}h} \tag{2}$$

while the magnitudes of the 2nd, 3rd and 4th harmonics may be determined by:

$$I_h = \frac{0.1S_{nom}}{\sqrt{3}U_{nom}h}, \tag{3}$$

where S_{nom} is the rated power of supply transformer and kVA, U_{nom} is rated voltage of the power supply system.

In [44], the rectifier is represented by a simplified single-line diagram, which is used to describe the transfer functions of the converter model. In this case, two transfer functions are used to describe the model. These functions relate the DC and AC sides of the converter, taking into account the variation of the firing angle and commutation overlap.

According to IEEE Std 519-2014, the harmonic currents on the AC side are determined by Equation (1), assuming that the direct current of the bridge rectifier has no ripple. However, due to commutation phenomena, the shape of the current consumed by the rectifier takes on a different form. In this case, the harmonic currents of three-phase rectifiers can be determined by the equation:

$$I_h = I_{dc}\left\{\sqrt{\frac{6}{\pi}}\cdot\frac{\sqrt{A^2+B^2-2AB\cos(2\alpha+\mu)}}{h[\cos\alpha-\cos(\alpha+\mu)]}\right\} \tag{4}$$

where α is a firing angle and μ is a commutation overlap angle. Coefficients A and B are determined by the equations:

$$A = \frac{\sin\left[(h-1)\frac{\mu}{2}\right]}{h-1},\ B = \frac{\sin\left[(h+1)\frac{\mu}{2}\right]}{h+1} \tag{5}$$

When determining the parameters of the equivalent nonlinear electrical load according to IEC/TR 61000-3-6-2020, the general law of summation for harmonic voltage and current can be empirically adopted. The law for the resulting harmonic current of order h is expressed by the equation:

$$I_h = \sqrt[\beta]{\sum_i I_{hi}^{\beta}} \tag{6}$$

where I_h is the value of the h-order resulting harmonic current for the considered set of sources (probabilistic value), I_{hi} are the values of various h-order individual emission levels that should be combined, and β is an index determined by IEC/TR 61000-3-6-2020. A similar formula is proposed to be used for harmonic voltage summation.

Obviously, existing methods make it possible to determine the parameters of a nonlinear electrical load with a certain margin of error, which increases when taking into account the grid parameters, equipment loading and simulating equivalent loads. In such cases, difficulties often arise, since data regarding power supply systems may be outdated or insufficient, and the number of outgoing cable lines at the point of equivalent can be very large. Thus, the purposes of this work are to experimentally determine the parameters of nonlinear loads of various types, and to develop a new method for determining the parameters of an equivalent nonlinear electrical load.

2. Research Methods

2.1. Laboratory Test Bench

The study was carried out using a laboratory test bench that included the following: a connection point to the energy system with a phase to phase voltage of 380 V; variable grid inductance L, connected to the energy system in series; an uncontrolled rectifier (UR) loaded with variable resistance R_{UR} and unregulated inductance L_{UR} in DC link; a thyristor rectifier (TR) loaded with resistive element R_{TR} in DC link; and a thyristor power regulator (TPR) with resistance load R_{TPR}.

The laboratory test bench electrical scheme is presented in Figure 1. The electrical load can be connected both individually and simultaneously. Variation of the uncontrolled rectifier parameters was achieved by changing the parameters of the DC link, while variation of the thyristor rectifier and power regulator parameters was achieved by changing the firing angle of the thyristors.

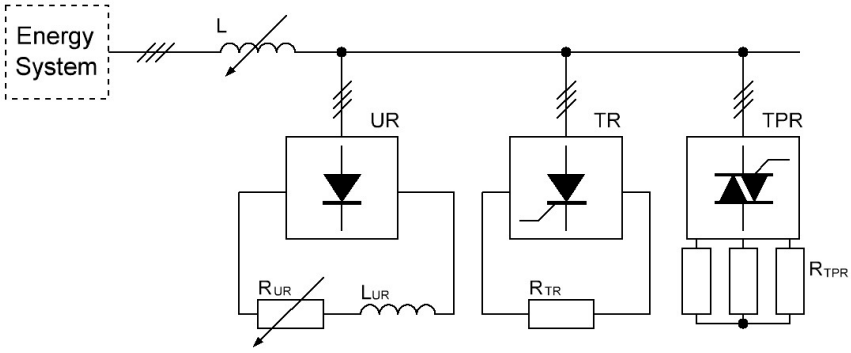

Figure 1. Schematic of the laboratory test bench.

The electrical load parameters are presented in Table 1.

Table 1. The parameters of the laboratory equipment.

Elements of the Scheme	Parameters and Values
Grid/system parameters	Us = 380 V, L = 0 ± 4 mH
Uncontrolled rectifier (UR)	U_{UR} = 380 V, R_{UR} = 42 ± 176 Ω, L_{UR} = 40 mH
Thyristor rectifier (TR)	U_{TR} = 380 V, P_{TR} = 0.5 ± 4.0 kW
Thyristor power regulator (TPR)	U_{TPR} = 380 V, P_{TPR} = 0.5 ± 4.0 kW

In the first stage, the study was carried out with nonlinear loads separately connected to the energy system. During the experiment, parameter L was changed according to the values L_0 = 0 mH, L_1 = 1 mH, L_2 = 4 mH, and the parameters of nonlinear loads were changed according to the data presented in Table 1. During the experiment, current and voltage waveforms were recorded for various laboratory test bench modes. Further, data processing was carried out, from which the magnitudes of the current and voltage harmonics, the spectrum of harmonics, as well as the phase shift angles at harmonic frequencies were obtained. Measurements were carried out using a Rigol DS2202A oscilloscope. In the second stage, all nonlinear loads were connected to the point of common coupling simultaneously, and the parameters of grid inductance were changing, similar to the first stage of the experiment. Also, data on the current and voltage waveforms of the aggregated load were recorded, including the magnitudes and the phase shift angles at harmonic frequencies.

The obtained experimental data were compared with the analytical expressions described in Section 1. In this case, the current harmonic magnitudes of the individual nonlinear loads such as UR were compared with Equation (1), the TPR with Equations (2) and (3), and the TR with Equation (4). The current harmonic magnitudes of the aggregated nonlinear loads were compared with Equation (5).

2.2. Method of Determination the Parameters of Nonlinear Electrical Load

In this paper, a method is proposed for determining the parameters of a nonlinear electrical load based on the use of resonant shunt filters of harmonic currents. When a shunt filter tuned to any frequency with h order is connected to the point of common coupling, the harmonic current generated by this nonlinear electrical load I_{NLh} flows through this shunt filter as current I_{Fh} at a tuned harmonic frequency (Figure 2).

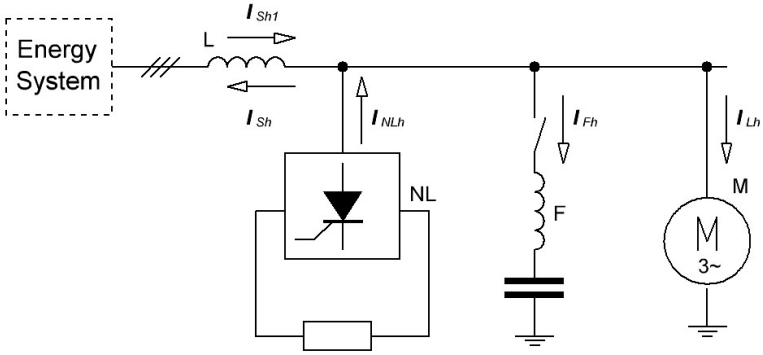

Figure 2. Scheme for the method of determination of nonlinear load parameters.

In this case, the value of current I_F was determined by the adjustment of filter parameters. Ideally, the harmonic current of nonlinear load I_{NLh} at tuned frequency completely flows through the filter:

$$\bar{I}_{NLh} = \bar{I}_{Fh}. \tag{7}$$

In the case of inaccurate adjustment of the filter parameters, part of the harmonic current flows through the system impedance, and the other part through the filter circuit. Considering harmonic currents, the current flowing through a linear load I_{Lh} connected to the same point of common coupling is incommensurably small in comparison with the filter I_{Fh} and system currents I_{Sh} because the impedance of the linear load is rather more than the energy system and filter impedance at tuned frequency. Summing up these complex values, it is possible to determine the value of the nonlinear harmonic current, I_{NLh}, of the load:

$$\bar{I}_{NLh} = \bar{I}_{Fh} + \bar{I}_{Sh}. \tag{8}$$

This method is also efficient when the energy system is a source of harmonics. Then, the harmonic currents generated by outside nonlinear consumers flow through this filter. To exclude their influence on the determination of the nonlinear load parameters, it is necessary to provide measurements of the energy system harmonic current. Then, subtracting the values of the harmonic currents flowing from the grid side I_{Sh1}, it is possible to determine the values of the nonlinear load currents:

$$\bar{I}_{NLh} = \bar{I}_{Fh} - \bar{I}_{Sh1} \tag{9}$$

The proposed method works under the assumption that the source of harmonics is presented in the form of current sources. However, when a harmonic shunt filter is connected to the point of common coupling, the instantaneous current of the nonlinear load may change. In other words, the spectrum and magnitudes of current harmonics generated by the nonlinear load may change. In this work, to verify this assumption, experimental studies were carried out using a shunt filter on the 5th and 7th harmonics. During the experiment, the current of various nonlinear load types was compared before and after the shunt filter was connected. The filter parameters are presented in Table 2.

Table 2. The parameters of shunt filter.

Parameter	Value
Resistance of the 5th and 7th harmonic filter	0.2 Ω
Inductance of the 5th and 7th harmonic filter	8.29 mH
Capacitance of the 5th/7th harmonic filter	50/26 μF

3. Experimental Determination of Nonlinear Load Parameters of Various Types

3.1. Experimental Study of Individual Nonlinear Load Parameters

This experiment was carried out to determine the parameters of the harmonic currents of three different nonlinear loads separately connected to the point of common coupling, namely, UR with resistance and inductance in DC-link, TR with resistance in DC-link, TPR with electrical heating tubes. The experimental parameters were changed as described in Section 2.

Figure 3a shows waveforms of the UR currents at various values of the grid inductance (L_0 and L_2) and Figure 3b shows the relative values of the UR harmonic currents I_h/I_1 for different power consumption P and grid inductance L_2 equal to 4 mH.

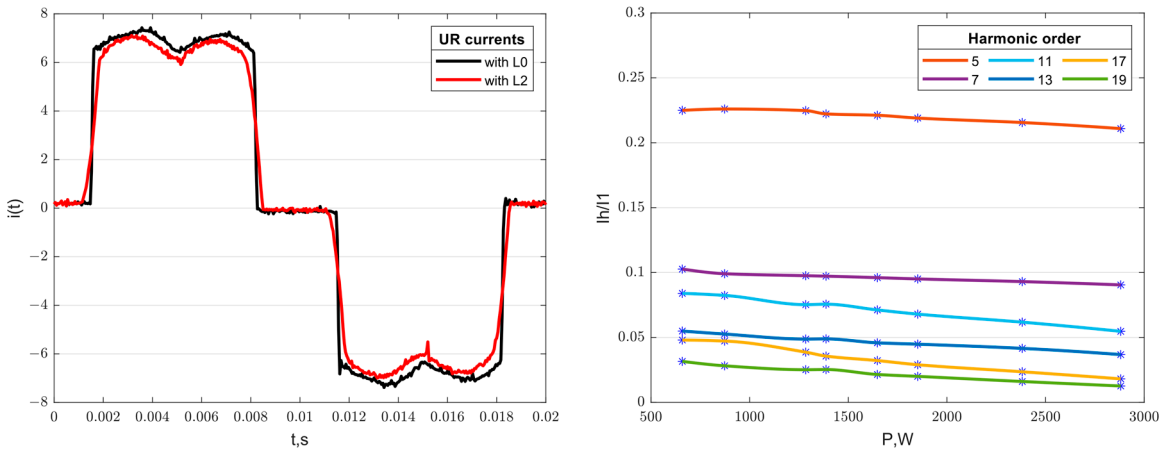

(**a**) (**b**)

Figure 3. Waveforms of the UR currents at various values of the grid inductance (**a**); relative values of the UR harmonic currents for different power consumption (**b**).

Figure 4a shows the waveforms of the TR currents at various values of the grid inductance (L_0 and L_2), and Figure 4b shows the relative values of the TR harmonic currents I_h/I_1 for different power consumption P with grid inductance L_2 equal to 4 mH.

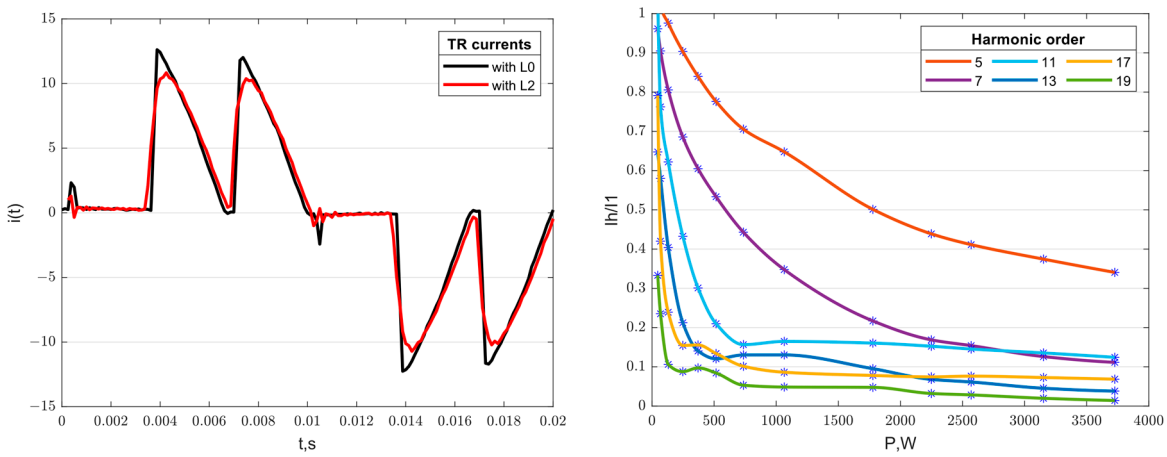

(**a**) (**b**)

Figure 4. Waveforms of the TR currents at various values of the grid inductance (**a**); relative values of the TR harmonic currents for different power consumption (**b**).

Figure 5a shows waveforms of the TPR currents at various values of the grid inductance (L_0 and L_2), and Figure 5b shows the relative values of the TPR harmonic currents I_h/I_1 for different power consumption P with grid inductance L_2 equal to 4 mH.

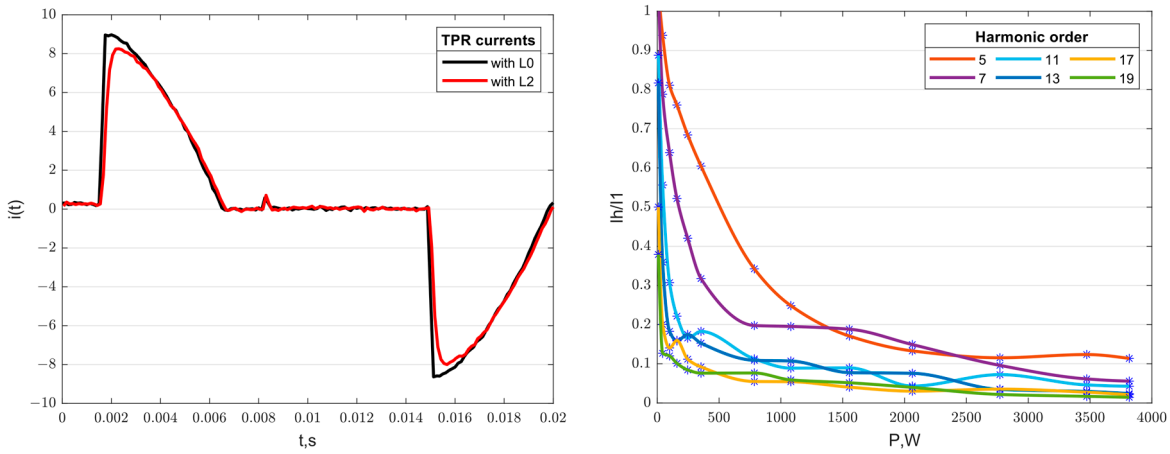

(**a**) (**b**)

Figure 5. Waveforms of the TPR currents at various values of the grid inductance (**a**); relative values of the TPR harmonic currents for different power consumption (**b**).

It can be concluded that connecting an additional grid inductance reduces the current harmonics generated by nonlinear loads, as can be seen in the presented current waveforms. However, the total harmonic distortion in current (THDI) decreases insignificantly for UR when additional inductance is connected (from 29% to 26%), and practically does not depend on the loading of equipment, as confirmed by the data shown in Figure 3. From Figure 4, it follows that THDI for TR in the absence of additional inductance was 44%, and with an additional inductance of L_2-39%. The harmonic composition of the consumed current for a thyristor rectifier has a significant dependence on the loading of equipment. So, THDI was 138% when the loading of electrical equipment was 10%, but dropped to 44% when the loading of equipment was increased to 90% in the absence of additional inductance. The trend of changing the parameters of current harmonics for TR is also typical for TRP, as confirmed by the data shown in Figure 5.

The dependencies of the phase shift angles at harmonic frequencies were obtained for various types of nonlinear load (Figure 6).

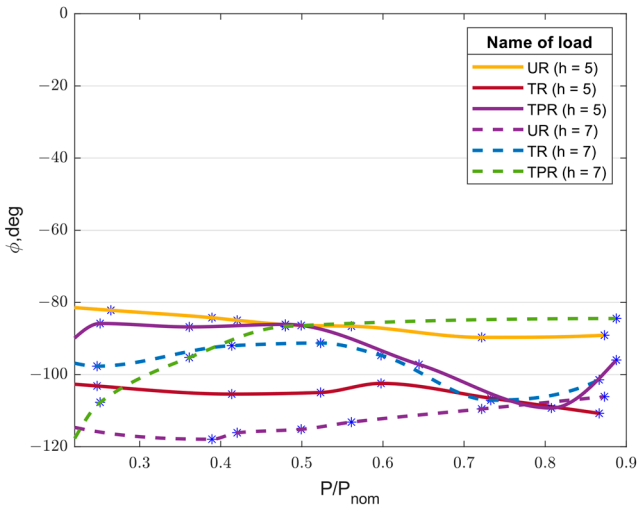

Figure 6. Phase shift angles at 5th and 7th harmonics for UR, TR and TPR.

It can be seen from Figure 6 that the phase shift angles for the 5th and 7th harmonics varies from −85 to −120° for various types of nonlinear loads. The minus sign means that the direction of current harmonics flow did not coincide with the direction of current flow at the fundamental frequency during measurements. So, the obtained values of phase shift angles characterized the active-inductive load and were determined by the energy

system parameters at the harmonic frequencies. In this case study, the connected additional grid inductance was crucial. As part of the experiment, a 3 Ohm resistance was connected to the supply line instead of an additional grid inductance. In this case, the phase shift angles for the 5th and 7th harmonics were about 180°, which is typical for the resistive character of the energy system parameters and for the generation of harmonic currents into the energy system (from consumer side to grid side). Thus, the phase parameters of a nonlinear load at harmonic frequencies were determined by the parameters of the energy system. It follows that when simulating an equivalent nonlinear load in the form of current sources, only their amplitudes can be specified. In this case, the phase shift angles at the harmonic frequencies will be determined by the energy system model. Therefore, only the values of the current harmonic magnitudes were compared with the existing analytical expressions in this study.

In accordance with the expressions specified in Section 2, the values of the current harmonic magnitudes for various types of nonlinear loads were determined and compared with the results of experimental measurements. The data on the calculated relative errors are presented in Table 3.

Table 3. Relative errors of the calculated and measured current harmonic magnitudes.

Type of the Load	Comparison Equation	5th Harmonic Error, %	7th Harmonic Error, %	11th Harmonic Error, %	13th Harmonic Error, %
UR	(1)	10.3	32.1	21.2	33.2
TPR	(2), (3)	27.9	32.5	38.1	24.2
TR	(4)	40.4	57.5	46.3	60

It can be concluded from the Table 3 that the relative error in calculating the values of the harmonic current magnitudes of various types of nonlinear load by analytical expressions in comparison with the measured data varied from 10% to 60%. It should be noted that lower order harmonic currents are determined with the smallest relative error. As such, the analytical model for determining the parameters of TR was the least accurate of the considered approaches.

3.2. Experimental Study of Aggregated Load Parameters

In this section, the experimental determination of the harmonic parameters of three nonlinear electrical loads simultaneously connected to the point of common coupling was considered. The experimental parameters were changed as described in Section 2. Figure 7 shows waveforms and harmonic spectrum of aggregated load currents at various values of grid inductance.

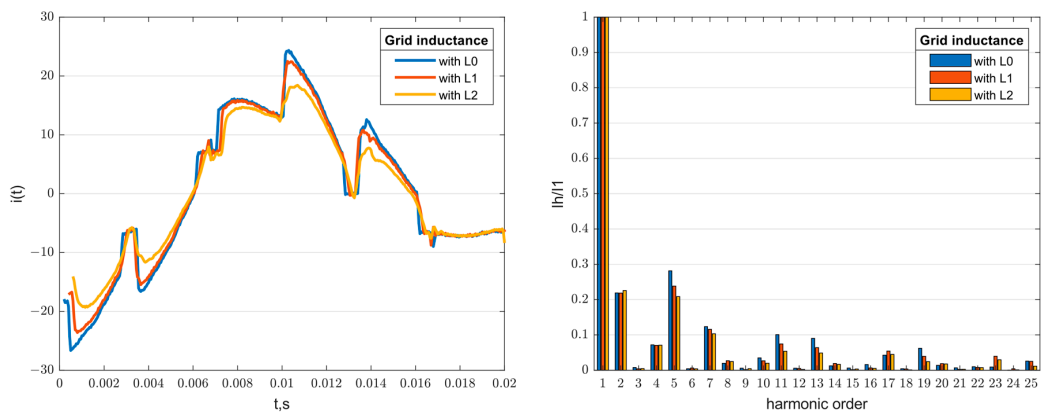

(**a**) (**b**)

Figure 7. Waveforms (**a**) and harmonic spectrum (**b**) of aggregated load currents.

Figure 7 also shows a tendency toward a decrease in harmonic currents with an increase in the system impedance. With a four-fold increase in grid inductance, the magnitudes of the 5th and 7th current harmonics decreased by 25 and 27%, respectively. A comparison of the 5th and 7th current harmonic magnitudes, obtained by expression (5) and measured during the experiment without additional grid inductances, showed that for the 5th harmonic, the relative error was 38%, and for the 7th harmonic, 54%. The relative error in estimating the current harmonic magnitudes with theoretical expressions increased in the presence of additional grid inductances. Due to the large values of the current relative errors, there was a need for a more accurate determination of the nonlinear electrical load parameters, including the methods based on real measurements.

4. Determination of Nonlinear Load Parameters Based on Measurements

4.1. Current Harmonics of Nonlinear Load When Filter Is Connected

An important condition for determining the parameters of a nonlinear electrical load is the constancy of the generated harmonic currents before and after connecting a passive harmonic filter in parallel with the load. To prove this, experimental studies were carried out on a laboratory test bench. The current harmonic magnitudes of various types of nonlinear load were measured before and after connecting a passive filter. The parameters of the passive filter are presented in Table 2. As an example, Figure 8 shows the waveforms and harmonic spectrum of UR currents before and after connecting the 5th harmonic filter with additional grid inductance L_1.

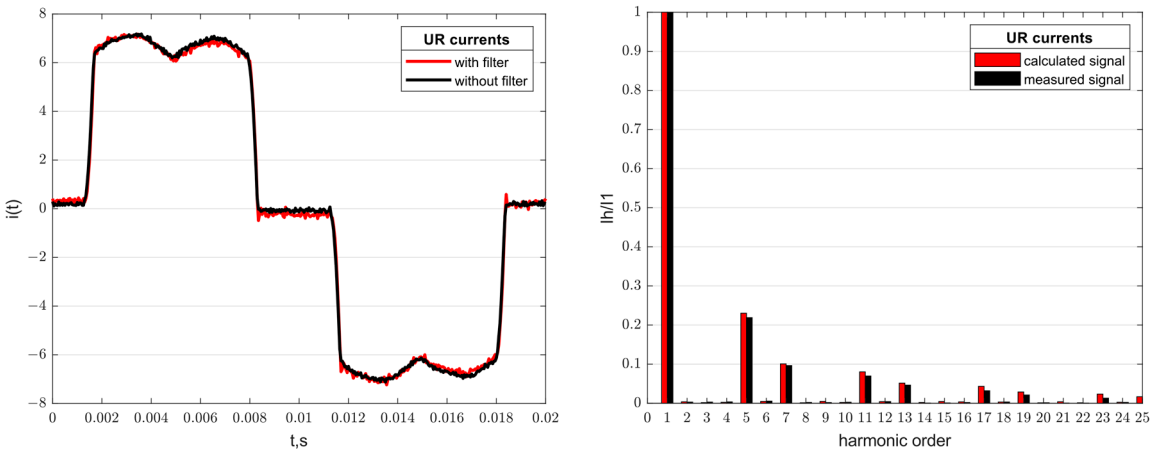

(**a**) (**b**)

Figure 8. The waveforms (**a**) and harmonic spectrum (**b**) of UR currents.

Then, an assessment of the relative error for various types of nonlinear load was carried out for different values of the additional grid inductance (L_0, L_1, L_2). Table 4 shows the errors in determining the current harmonic magnitudes relative to the magnitude at the fundamental frequency before and after connecting the filter of the 5th and 7th harmonics.

Table 4. The error of determination the current harmonic magnitudes via passive filter.

Type of the Load	Line Parameters	5th Harmonic Error, %	7th Harmonic Error, %
UR	$L_0\backslash L_1\backslash L_2$	3.5\1.0\4.7	2.2\2.7\4.0
TRP	$L_0\backslash L_1\backslash L_2$	2.9\0.2\8.1	3.2\0.2\2.3
TR	$L_0\backslash L_1\backslash L_2$	1.4\1.7\7.3	2.2\0.9\10.2

From the data presented in the Table 4, it can be seen that the relative errors of determination the current harmonic magnitudes did not exceed 5% for cases with additional grid inductances L_0 and L_1, which is typical for low-voltage networks of centralized power supply systems. In the case of connecting the grid inductance L_2, the current harmonic

magnitudes before and after connecting the passive filter varied within 10%. At the same time, total harmonic distortion in voltage (THDU) was about 13%, which is a rather high value of distortion for low-voltage networks and could affect the error in determining the current harmonic magnitudes. It should be noted that the determination of the current harmonic magnitudes with an error of 10% is a reasonably good result when calculating the operation modes with harmonic distortions.

4.2. Current Harmonics of Aggregated Nonlinear Loads When Filter Is Connected

It was found that the harmonic currents generated by the individual nonlinear electrical loads, connected to the power supply system, did not change significantly when a passive harmonic filter was connected. So, in the presence of a large number of nonlinear electrical loads connected to the consumer busbars, it is possible to correctly determine the parameters of an equivalent nonlinear load based on measurements using a resonant shunt filter. The proposed method was tested on a laboratory test bench (Figure 1) with different nonlinear electrical loads connected. The parameters of the loads are listed in Table 1. At the same time, the parameters of the additional grid inductance were varied. As an example, Figure 9 shows waveforms and harmonic spectrum of aggregated load current (UR and TR are connected) before and after connecting a passive 5th harmonic filter for grid inductance L_2. The value of the equivalent load harmonic current I_{NLh} after connecting the filter was determined by Equation (7) as the sum of the system harmonic current I_{Sh} and the harmonic filter current I_{Fh} for each harmonic separately.

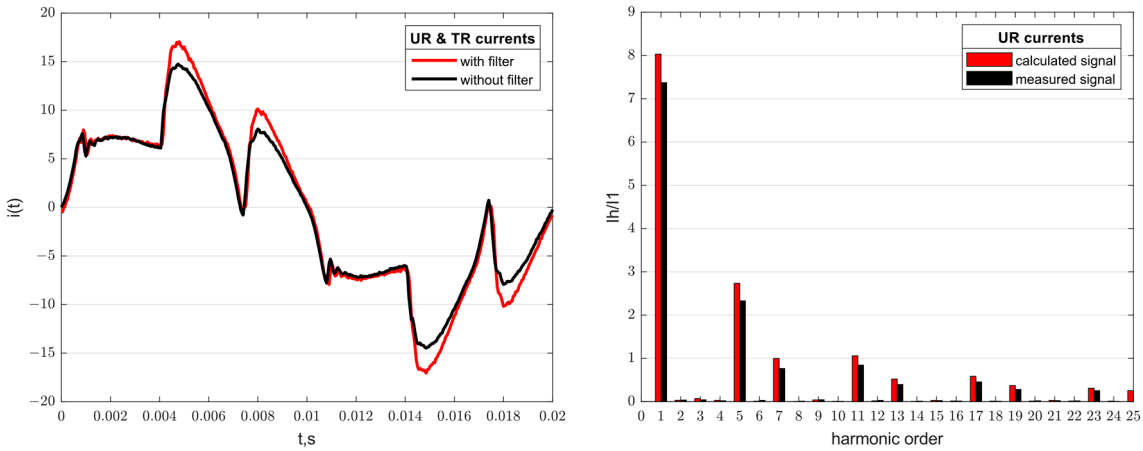

(**a**) (**b**)

Figure 9. The waveforms (**a**) and harmonic spectrum (**b**) of aggregated load currents with filter.

Figure 9 shows a minor difference in the current waveforms, which was associated with an insignificant voltage change after connecting the passive filter. Further, the error in determining the 5th harmonic current magnitude relative to the current magnitude at the fundamental frequency was estimated for a different composition of nonlinear loads and different values of grid inductance. Table 5 shows the data of the relative errors of the 5th harmonic current magnitude before and after the connection of the 5th harmonic filter.

Table 5. The 5th current harmonic relative error of the equivalent nonlinear load.

Line Parameters	Relative Error, %		
	UR + TR	UR + TR + TRP	TR + TRP
L_0	1.23	3.92	0.94
L_1	3.53	3.82	3.52
L_2	7.25	13.94	12.49

From the data presented in the table, it can be seen that the relative errors of determination the current harmonic magnitudes of the equivalent load did not exceed 5% when the parameters of grid inductance were equal to L_0 and L_1. This corresponds to the results for separately connected nonlinear loads. With a four-fold increase in grid inductance, the error in estimating the current harmonic magnitudes of the equivalent load increased to 14%. However, the error remained acceptable for calculating the operating modes in the presence of harmonic distortions.

5. Discussions

Thus, the parameters of different types of nonlinear electrical loads have been identified by carrying out measurements on a laboratory test bench in the study. The obtained current harmonic magnitudes were compared with the values calculated according to the well-known analytical expressions for these types of load. The relative error for the individual nonlinear consumers reached 60%, and 54% for the equivalent nonlinear electrical load under laboratory conditions. The relative error increased in the presence of additional grid inductances and different equipment loading.

The method has been proposed for determining the parameters of a nonlinear electrical load based on the use of harmonic shunt filters. This method makes it possible to determine the current harmonic magnitudes of both individual and equivalent nonlinear electrical loads by measuring the currents of the energy system and the filter. It has been shown that the spectrum and magnitudes of the nonlinear load currents remained almost constant, regardless of the harmonic filter connection. Furthermore, the maximum relative error in determining the harmonic current magnitudes of the equivalent nonlinear load did not exceeded 14% before and after connecting the filter. Some factors should be highlighted that can affect the determination of the harmonic current parameters of the equivalent nonlinear electrical load:

- influence of linear electrical load
- influence of resonance phenomena
- influence of harmonics generated from the grid side.

Let's comment on the points outlined above. The parameters of a linear electrical load, such as asynchronous motors, are represented by resistance and inductance, the values of which turn out to be much higher than the impedance of the tuned filter and the energy system at the harmonic frequencies. Therefore, the calculation of the current harmonic magnitudes of the converters cannot be significant influenced by the parameters of the linear electrical load.

Resonance phenomena are possible if there are harmonics in the spectrum whose frequencies are lower than the frequency of the tuned filter. In this case, it is possible that the voltage increases at the harmonic frequency. This can affect the current harmonic magnitude of the converter at the considered harmonic frequency. Therefore, it is recommended to select the filter parameters starting with the lowest harmonic frequency presented in the power supply system spectrum. However, even in this case, the current harmonic magnitudes of the converter can be correctly determined at the tuned frequency of the filter. If the filter is incorrectly configured or the filter parameters are changed during operation, series resonance with the network impedance is possible. However, incorrect filter settings are excluded, since, in fact, the filter is a measuring device, the parameters of which must be strictly controlled prior to connection. Changing the filter parameters as a result of long-term operation is also excluded, since the measuring filter is connected for several days that covers various modes of nonlinear load operation.

Additional grid side harmonic currents can flow through the passive filter. Then, according to the superposition method, the harmonic current of the input feeder generated from the consumer side decreases, since its direction is opposite to the harmonic current generated from the grid side. However, in this case, the decrease in the mentioned harmonic current is compensated by an increase in the filter harmonic current on the same value. Therefore, the value of the current harmonic magnitude of the nonlinear load does not change.

6. Conclusions

As a result of the studies, a new method for evaluating the parameters of nonlinear electrical load was developed based on the application of a harmonic filter. The developed method was compared with existing analytical expressions, and it was shown that the error in determining the magnitudes of current harmonics was reduced by approximately four times.

To implement this method, it is necessary to measure the harmonic currents of the energy system and harmonic filter. Then, depending on the direction of the energy system harmonic current, the current harmonic magnitude of the nonlinear load is determined. This method makes it possible to accurately assess the current harmonic magnitudes of the equivalent nonlinear load, which can be connected in large quantities to consumer buses. The obtained values of the current harmonic magnitudes can be used in the modeling of a nonlinear electrical load as a current source. Data on the daily change in the current harmonic magnitudes of the nonlinear load make it possible to calculate power quality indicators at minimum, average and maximum values of current distortions.

Further research will include the development of a method for selecting the parameters of harmonic filter to improve the accuracy of determining the current harmonic magnitude of the nonlinear load. It is also planned to create a mobile measuring device based on the developed method for implementation in networks with a voltage of 0.4 kV.

Author Contributions: Conceptualization, A.S.; methodology, A.S. and Y.S.; investigation, I.D. and V.D.; writing—original draft preparation, A.S.; supervision and project administration, A.S. and Y.S.; writing—review and editing, Y.S. and V.D. All authors have read and agreed to the published version of the manuscript.

Funding: This research was financially supported by the subsidy for the state assignment in the field of scientific activity for 2021 No. FSRW-2020-0014 (Sections 1–3) and the Russian Science Foundation grant No. 21-79-10027, https://rscf.ru/en/project/21-79-10027 (Sections 4 and 5).

Institutional Review Board Statement: Not applicable.

Informed Consent Statement: Not applicable.

Conflicts of Interest: The authors declare no conflict of interest.

References

1. Vasilyev, B.Y.; Shpenst, V.A.; Kalashnikov, O.V.; Ulyanov, G.N. Providing energy decoupling of electric drive and electric grids for industrial electrical installations. *J. Min. Inst.* **2018**, *229*, 41–49. [CrossRef]
2. Simiyu, P.; Davidson, I.E. MVDC railway traction power systems; state-of-the art, opportunities, and challenges. *Energies* **2021**, *14*, 4156. [CrossRef]
3. Veprikov, A.A.; Abramovich, B.N. Prospects for IGBT application in electrical power converters for industrial high-current DC loads. *IOP Conf. Ser. Mater. Sci. Eng.* **2019**, *560*, 012131. [CrossRef]
4. Ahmad, Z.; Torres, J.R.; Kumar, N.V.; Rakhshani, E.; Palensky, P.; van der Meijden, M. A power hardware-in-the-loop based method for FAPR compliance testing of the wind turbine converters control. *Energies* **2020**, *13*, 5203. [CrossRef]
5. Janardhan, K.; Mittal, A.; Ojha, A. Performance investigation of stand-alone solar photovoltaic system with single phase micro multilevel inverter. *Energy Rep.* **2020**, *6*, 2044–2055. [CrossRef]
6. Bi, K.; Liu, Y.; Zhu, Y.; Fan, Q. An impedance source modular DC/DC converter for energy storage system: Analysis and design. *Int. J. Electr. Power Energy Syst.* **2021**, *133*, 107261. [CrossRef]
7. Zheng, L.; Kandula, R.P.; Divan, D. Soft-switching solid-state transformer with reduced conduction loss. *IEEE Trans. Power Electron.* **2021**, *36*, 5236–5249. [CrossRef]
8. Belsky, A.A.; Morenov, V.A.; Kupavykh, K.S.; Sandyga, M.S. Wind turbine electrical energy supply system for oil well heating. *Energ. Proc. CIS High. Educ. Inst. Power Eng. Assoc.* **2019**, *62*, 146–154. [CrossRef]
9. Shklyarskiy, Y.; Skamyin, A.; Vladimirov, I.; Gazizov, F. Distortion load identification based on the application of compensating devices. *Energies* **2020**, *13*, 1430. [CrossRef]
10. Lavrik, A.; Zhukovskiy, Y.; Tcvetkov, P. Optimizing the size of autonomous hybrid microgrids with regard to load shifting. *Energies* **2021**, *14*, 5059. [CrossRef]
11. Zhang, L.; Xie, Y.; Ye, J.; Xue, T.; Cheng, J.; Li, Z.; Zhang, T. Intelligent frequency control strategy based on reinforcement learning of multi-objective collaborative reward function. *Front. Energy Res.* **2021**, *9*, 587. [CrossRef]
12. Belsky, A.; Dobush, V.S.; Haikal, S.F. Operation of a single-phase autonomous inverter as a part of a low-power wind complex. *J. Min. Inst.* **2019**, *239*, 564–569. [CrossRef]

13. Zamyatin, E.; Voytyuk, I.; Zamyatina, E. Increasing the energy efficiency of an enterprise by point compensating of power quality distortions. *E3S Web Conf.* **2019**, *140*, 04010. [CrossRef]
14. Munoz-Guijosa, J.M.; Kryltcov, S.B.; Solovev, S.V. Application of an active rectifier used to mitigate currents distortion in 6–10 KV distribution grids. *J. Min. Inst.* **2019**, *236*, 229–238. [CrossRef]
15. Du, X.; Zhou, L.; Lu, H.; Tai, H.M. DC link active power filter for three-phase diode rectifier. *IEEE Trans. Ind. Electron.* **2012**, *59*, 1430–1442. [CrossRef]
16. SHidlovskij, A.K.; ZHarkin, A.F. *High Harmonics in Low-Voltage Electrical Networks*; Naukova Dumka: Kiev, Ukraine, 2005; ISBN 966-00-0471-0.
17. Carpinelli, G.; Iacovone, F.; Russo, A.; Varilone, P.; Verde, P. Analytical modeling for harmonic analysis of line current of VSI-fed drives. *IEEE Trans. Power Deliv.* **2004**, *19*, 1212–1224. [CrossRef]
18. Lian, K.L.; Perkins, B.K.B.K.; Lehn, P.W. Harmonic analysis of a three-phase diode bridge rectifier based on sampled-data model. *IEEE Trans. Power Deliv.* **2008**, *23*, 1088–1096. [CrossRef]
19. Li, F.; Wang, Y.; Wu, F.; Huang, Y.; Liu, Y.; Zhang, X.; Ma, M. Review of real-time simulation of power electronics. *J. Mod. Power Syst. Clean Energy* **2020**, *8*, 796–808. [CrossRef]
20. Xie, Q.; Shi, G. An analytical gm/ID-based harmonic distortion prediction method for multistage operational amplifiers. *Int. J. Circuit Theory Appl.* **2021**, *49*, 2047–2073. [CrossRef]
21. Abramovich, B.N. Uninterruptible power supply system for mining industry enterprises. *J. Min. Inst.* **2018**, *229*, 31. [CrossRef]
22. Estrada, L.; Vázquez, N.; Vaquero, J.; de Castro, Á.; Arau, J. Real-time hardware in the loop simulation methodology for power converters using labview FPGA. *Energies* **2020**, *13*, 373. [CrossRef]
23. Gurrala, G.; Batageri, A.; Dinesha, D.L. Real-time simulation of power converters using adomian decomposition method on mini-FSS. In Proceedings of the 2016 IEEE International Conference on Power Electronics, Drives and Energy Systems (PEDES), Trivandrum, India, 14–17 December 2017; pp. 1–6. [CrossRef]
24. Hansen, S.; Asiminoaei, L.; Blaabjerg, F. Simple and advanced methods for calculating six-pulse diode rectifier line-side harmonics. In Proceedings of the 38th IAS Annual Meeting on Conference Record of the Industry Applications Conference, Salt Lake City, UT, USA, 12–16 October 2003; Volume 3, pp. 2056–2062. [CrossRef]
25. ZHezhelenko, I.V. *High Harmonics in Electrical Systems of Industrial Enterprices*; Energoatomizdat: Moscow, Russia, 1984.
26. Katic, V.A. A new method of three-phase bridge rectifier current and a new method of three-phase bridge rectifier current and voltage harmonics determination. *J. Power Energy Syst.* **1994**, *14*, 44–48.
27. Grötzbach, M.; Redmann, R. Analytical predetermination of complex linecurrent harmonics in controlled ac/dc converters. *IEEE Trans. Ind. Appl.* **1997**, *33*, 601–612. [CrossRef]
28. Rice, D.E. A detailed analysis of six-pulse converter harmonic currents. *IEEE Trans. Ind. Appl.* **1994**, *30*, 294–304. [CrossRef]
29. Gentile, T.; Grady, M.; El-Hawary, M.E.; Halpin, M.; Xu, W.; Ranade, S.; Ribeiro, P.F. *Tutorial on harmonics modeling and Simulation*; IEEE Power Engineering Society: Piscataway, NJ, USA, 1998.
30. Ranade, S.; Xu, W. Task force on harmonics modeling and simulation harmonics working modeling and simulation of the propagation of harmonics in electric power networks: Part I. Concepts, models, and simulation techniques. *IEEE Trans. Power Deliv.* **1996**, *11*, 452–465.
31. Lee, J.; Kwon, Y.C.; Sul, S.K. Identification of IPMSM flux-linkage map for high-accuracy simulation of IPMSM drives. *IEEE Trans. Power Electron.* **2021**, *36*, 14257–14266. [CrossRef]
32. Mayordomo, J.G.; Beites, L.F.; Yang, X.; Xu, W. A detailed procedure for harmonic analysis of three-phase diode rectifiers under discontinuous conduction mode and nonideal conditions. *IEEE Trans. Power Deliv.* **2018**, *33*, 741–751. [CrossRef]
33. Li, Y.; Wang, W.; Yuwen, B.; Wei, S.; Su, W.; Lu, Z. Harmonic model and propagation in power system: A review. In Proceedings of the IECON 2019—45th Annual Conference of the IEEE Industrial Electronics Society, Lisbon, Portugal, 14–17 October 2019; pp. 6147–6151. [CrossRef]
34. Grbtzbach, M.; Redmann, R. Line current harmonics of VSI-Fed adjustable speed drives. *IEEE Trans. Ind. Appl.* **2000**, *36*, 683–690. [CrossRef]
35. Maksimovic, D.; Stankovic, A.M.; Joseph Thottuvelil, V.; Verghese, G.C. Modeling and simulation of power electronic converters. *Proc. IEEE* **2001**, *89*, 898–912. [CrossRef]
36. Mayordomo, J.G.; Carbonero, Á.; Beites, L.F.; Asensi, R.; Xu, W. A contribution towards a general and systematic procedure for modeling line commutated AC/DC converters in the harmonic domain. *IEEE Trans. Power Deliv.* **2009**, *24*, 2415–2427. [CrossRef]
37. Bolsens, B.; De Brabandere, K.; Van Den Keybus, J.; Driesen, J.; Belmans, R. Model-based generation of low distortion currents in grid-coupled PWM-inverters using an LCL output filter. *IEEE Trans. Power Electron.* **2006**, *21*, 1032–1040. [CrossRef]
38. Smith, B.C.; Watson, N.R.; Wood, A.R.; Arrillaga, J. A sequence components model of the ac/dc converter in the harmonic domain. *IEEE Trans. Power Deliv.* **1997**, *12*, 1736–1743. [CrossRef]
39. Smith, B.C.; Arrillaga, J.; Wood, A.R.; Watson, N.R. A review of iterative harmonic analysis for AC-DC power systems. *IEEE Trans. Power Deliv.* **1998**, *13*, 180–185. [CrossRef]
40. Baghzouz, Y. An accurate solution to line harmonic distortion produced by ac/dc converters with overlap and dc ripple. *IEEE Trans. Ind. Appl.* **1993**, *29*, 536–540. [CrossRef]
41. Grötzbach, M.; Ried, C. Investigation of AC/DC converter harmonics by an analytical based time-discrete approach. *IEEE Trans. Power Deliv.* **1997**, *12*, 874–880. [CrossRef]

42. Jopri, M.H.; Ab Ghani, M.R.; Abdullah, A.R.; Manap, M.; Sutikno, T.; Too, J. K-nearest neighbor and naïve Bayes based diagnostic analytic of harmonic source identification. *Bull. Electr. Eng. Inform.* **2021**, *9*, 2650–2657. [CrossRef]
43. Faifer, M.; Laurano, C.; Ottoboni, R.; Toscani, S.; Zanoni, M. Frequency-domain nonlinear modeling approaches for power systems components—A comparison. *Energies* **2020**, *13*, 2609. [CrossRef]
44. Burch, R.; Chang, G.; Dwyer, R.; Grady, M.; Halpin, M.; Hatziadoniu, C.J.; Liu, Y.; Marz, M.; Medina-Rios, A.; Middledanff, S.; et al. Task force on harmonics modeling and simulation harmonics working group characteristics and modeling of harmonic sources—Power electronic devices. *IEEE Trans. Power Deliv.* **2001**, *16*, 791–800.